行政院國家科學委員會補助專題研究計畫 □ 成 果 報 告
■期中進度報告

銻化物基材之量子結構及元件（1/3）
Antimonide based quantum structures and devices

計畫類別：■ 個別型計畫　□ 整合型計畫
計畫編號：NSC　96－2221－E－009－221－
執行期間：　96　年　8　月　1　日至　97 年　7 月　31　日

計畫主持人：李建平教授　國立交通大學電子工程學系
共同主持人：
計畫參與人員：羅明城、凌鴻緒　國立交通大學電子工程學系

成果報告類型(依經費核定清單規定繳交)：■精簡報告　□完整報告

本成果報告包括以下應繳交之附件：
□赴國外出差或研習心得報告一份
□赴大陸地區出差或研習心得報告一份
□出席國際學術會議心得報告及發表之論文各一份
□國際合作研究計畫國外研究報告書一份

處理方式：除產學合作研究計畫、提升產業技術及人才培育研究計畫、列管計畫及下列情形者外，得立即公開查詢
□涉及專利或其他智慧財產權，□一年□二年後可公開查詢

執行單位：國立交通大學電子工程學系

中　華　民　國　97 年　6 月　1 日

一、 中文摘要

本年度的研究計畫我們針對兩方面做了深入的探討。首先我們研究了銻化鎵沾濕層之分散原子能階之發光特性，我們成功的觀察到一、二、三層銻化鎵原子沾濕層之光激光譜，藉由此不同發光之能量大小而計算出銻化鎵\砷化鎵兩種材料之價帶井深能量差異，我們推導出此第二類超晶格價電帶井深差異為 0.45 電子伏特。此外，我們也探討了銻原子對於高壓縮應力砷化銦鎵薄膜成長的介面活性效應。適當選取銻原子摻雜濃度，我們成功成長出 83%之高成分銦含量之砷化銦鎵二維電子氣結構。此結構在室溫下具有達 12500 $cm^2/V*sec$ 之電子遷移率。

關鍵詞：銻化鎵、沾濕層、價電帶井深差異

Abstrate

Discrete atomic layers of GaSb for the wetting layer prior to quantum dot formation give rise to transition peaks corresponding to quantum wells with one, two and three monolayers. From the transition energies we were able to deduce the band offset parameter between GaSb and GaAs. By fitting the experimental data with the theoretical calculated result using an 8×8 **k•p** Burt's Hamiltonian along with the Bir-Picus deformation potentials, the strain-free (fully-strained) valence band discontinuity for this type II heterojunstion was determined to be 0.45 eV (0.66 eV). Besides, the surfactant effect of Sb on the growth of highly-strained InGaAs layer was also investigated. With appropriate doping concentration of Sb, high In content (83%) InGaAs channels for the 2-dimensional electron gas (2DEG) were obtained. The room-temperature mobility of electron in this structure reaches 12500 $cm^2/V*sec$.

Keyword: GaSb, Wetting layer, Valance band offset

Introduction

III-antimonide compounds have been regarded as potential materials for applications in ultra high-speed devices and long-wavelength photonic devices due to their high electron mobility and small bandgap energies [1], [2]. Moreover, heterostructures composed of antimonides and other III-V compounds, such as arsenides, have also been of physical interest because of the unconventional type-II and type-III band alignment [3]-[5]. There have been lots of theoretical predictions for interesting optical, electronic, and magnetic phenomena in nanostructures with antimonides [6]. Recently, with the advances in epitaxy technology, such nanostructures have been grown with high quality and from them many interesting experimental findings, either predicted or sometimes unexpected, have been observed. For instance, quantum wells (QWs) and self-assembled quantum dots (QDs) made by GaSb embedded in GaAs matrix, because of type-II heterostructures, can provide an opportunity for observation of optical transition between spatially separate electrons and holes around the hetero-interfaces. However, despite of a large amount of effort being put in this material system, one of the most important parameters, the band offset between GaSb and GaAs has yet to be accurately determined. The wide range of reported value in this parameter often leads to ambiguous interpretation of experimental results and theoretical predictions for nanostructures made from this system.

High electron mobility device become more important in the IC technology. InAs has

smaller electron effective mass and thus higher electron mobility than GaAs or InP. Due to the expensive price of the InAs substrate, we try to grow the high indium composition InGaAs quantum well (QW) on the InP substrate. When the indium composition is too high or the InGaAs QW thickness is too large, there will be many dislocation generated in the InGaAs QW. In order to confine the electron wavefunction, the 10nm InGaAs QW is necessary. In previous study, it is difficult to increase the indium composition more than 70%. In our study, we use surfactant effect of antimony atom to increase the indium composition of the InGaAs QW. The electron mobility in this InGaAs channel at room temperature is elevated to 12500 cm^2/Vs with appropriate Sb beam flux.

Discrete monolayer light emission from GaSb wetting in GaAs

We report the study on optical transitions from monolayer-scale GaSb/GaAs QWs. Several distinct emission peaks were observed simultaneously from more than one sample by photoluminescence (PL) measurement. Each of the emission peaks lies at a definite position and can be well assigned to an optical transition from the QW of one, two, or three monolayers (MLs). Such definite transition energies allow us to determine the band offset between GaSb and GaAs by fitting the theoretical calculation to the measured data. Additionally, we also observed a subordinate emission peak that can be assigned to the optical transition in QDs. The QD emission can be observed only from the sample with a particular nominal GaSb thickness. Our study can therefore provide an insight into the mechanism for the formation of GaSb/GaAs QDs by molecule beam epitaxy (MBE).

The GaSb/GaAs nanostructures were grown by a VECCO Gen-II solid source MBE system with valve cracker sources of antimony and arsenic on (001) GaAs substrates. Two samples were prepared with different nominal GaSb film thicknesses: 1) sample A has a 1-ML GaSb film, and 2) sample B has a 2-ML GaSb film. In both samples, the GaSb films were sandwiched between a 150-nm GaAs buffer layer and a 150-nm GaAs capping layer. After the capping layer growth, a GaSb film with the same thickness was grown on the surface for atomic force microscope (AFM) measurement. We used As_4 as the arsenic source instead of As_2 to avoid intermixing of Sb and As atoms during the growth process [7].

Fig. 1 (a) and (b) show the AFM images of samples A and B, respectively. The smooth surface of sample A clearly shows that one monolayer of GaSb is not enough for quantum dot formation. However, on the surface of sample B, which had a 2-ML GaSb film we can see clear images of quantum dots. The density of the dots is about 1.04×10^{10} cm^{-2} and the height and the diameter of QDs are in the ranges of 5~10 nm and 50~60 nm, respectively. The formation of dots implies that the strain of the GaSb film cannot be sustained pseudomorphically in GaAs when more than 1 ML of GaSb is deposited. This is obviously due to the large lattice mismatch (8%) between GaSb and GaAs. But as will be described in the following, because of the nature of epitaxial growth, 1 ML GaSb deposition does not mean that there is only one kind of quantum wells with thickness of 1 ML. Actually what we found in this work, the maximum thickness of GaSb wetting layer (or quantum well) is 3 ML.

The PL measurement of the two samples was performed at 15 K with a CW Ar laser as the excitation source. The excitation power was varied from 1 mW to 100 mW and the laser beam spot size was around 200 μm in diameter. The measured spectra of samples A and B are shown in Fig. 2 (a) and (b), respectively. For sample A (see Fig. 2 (a)), the dominant peak is A_1 at ~1.4 eV. At low excitation levels, this is the only peak observed. But when the excitation exceeds 100 mW, two additional peaks A_2 and A_3 at about 1.3 and 1.22 eV are

observed along with the main peak A_1. For sample B, the situation is more complicated. From Fig. 2 (b), one can see that the emission is dominated by the peak B_2 at ~1.3 eV at all excitation levels. With the excitation level increasing, the side peaks B_1 and B_3, at 1.22eV and 1.4eV respectively, become more obvious. It is noticed that the three peaks B_i for sample B appear exactly at the same positions of the peaks A_i for sample A (i=1,2,3). At the excitation of 100 mW, we also found a broad peak B_{QD} around 1.05 eV in the spectrum for sample B. This peak is absent from the spectra for sample A and should be attributed to optical transition in QDs.

The fact that the positions of the emission peaks from two different samples are identical indicates that they originate from optical transitions in QWs with the same thickness. The fact that the QW in sample A has a nominal thickness of 1 ML allows us to assign the main peak A_1 to the optical transition in 1-ML QWs. Consequently, the lower peaks A_2 and A_3 at lower energies can be assigned to optical transitions in 2- and 3-ML QWs, respectively.. Based on a similar argument, the main peak B_2 of sample B, which was deposited with 2 MLs of GaSb, is due to the optical transition in 2-ML QWs. The two side peaks B_1 and B_3, therefore, naturally come from optical transitions in 1- and 3-ML QWs, respectively. The emission peak from the quantum dots, B_{QD}, is obviously wider than those from the quantum wells. This is caused by the nonuniformity in the size of the QDs. In contrast, the emission peaks from the thin QWs are narrower.

Because of the spatial separation between electrons and holes in the type-II GaSb/GaAs heterostructures, the carrier recombination lifetime is long and the carrier density can significantly increase with the excitation power. It follows that the electric field, which is induced by the spatially separated electron-hole space charges, increases around the heterointerface with the excitation power. As illustrated in the inset of Fig. 3, the increased electric field causes an upward shift of the energy level in the triangular potential well on the GaAs side. The observed blue shift for the emission peaks from GaSb/GaAs heterostructures is usually proportional to the 1/3 power of the excitation level, which is consistent with the triangular well approximation for electrons in GaAs [2], [3]. Fig. 3 shows the energy positions of the emission peaks A_1 and B_2 as functions of the cubic root of the excitation power density. The upper and lower lines in the figure, corresponding to A_1 and B_2 respectively, show how the transition energies in the 1-ML and 2-ML QWs change with excitation power. As seen in the figure, the energy shift follows the 1/3-power dependence quite well.

The plot in Fig. 3 can be used to obtain the transition energies of 1-ML and 2-ML GaSb/GaAs QWs in the absence of the excitation by linear extrapolation of the lines to the y-axis. The obtained transition energy can be considered as the bandgap energy of GaSb/GaAs QWs at thermal equilibrium. The resulting band gap energy is 1.404 eV for 1-ML QW and 1.298 eV for 2-ML QW. For the 3-ML QW, we cannot adopt the extrapolation method described above since we lack a series of appreciable emission signals at low excitation levels. Instead, we estimate the band gap energy at thermal equilibrium for the 3-ML QW to be about the position in energy of the peak B_3 obtained from sample B at excitation of 70 mW. This may overestimate the band gap energy according to the band filling effect mentioned above, but because the heating effect can compensate part of the energy shift, we expect the error is reasonably small compared to the difference from the band gap energy of 1-ML or 2-ML QW.

Now that the band gap energies of 1-, 2-, and 3-ML QWs have been obtained by experiment, we can determine the band offset between GaSb and GaAs by fitting the theoretically calculated band gap to the experimentally obtained data with the band offset as

an adjusting parameter. To this end, we use the eight-band **k•p** model to calculate the valence band structures of GaSb/GaAs QW in the flat-band approximation for various values of band offset [8]. The strain effect is considered, assuming the GaSb is pseudomorphically grown on strain-free GaAs, using the Bir-Picus deformation potential theory. The parameters taken for calculation can be found in Ref. [9]. The calculated transition energy is then the difference between the GaAs conduction band edge and the first heavy-hole subband edge in the GaSb QW. Fig. 4 shows the calculated transition energy of 1-, 2-, and 3- ML GaSb QWs for a series of valence band offset (VBO) values, along with the data obtained from measurement, where VBO is the difference in valence band edge between fully-strained GaSb and strain-free GaAs. As can be seen, the variation of the transition energy with the QW thickness is quite consistent between the calculation and the measurement, proving the correctness of our previous assignment of the emission peaks to optical transition in QWs with definite monolayer-scale thickness. Comparison between the calculated and the measured data suggests that the VBO should lie in the range of 0.61~0.81 eV. The strain-free VBO should lie in the range of 0.4~0.6 eV. For the best fitting, the fully-strained VBO is 0.66 eV and the strain-free VBO is 0.45 eV. The slight deviation in the calculated data is attributed to the omission of band bending in our calculation, which is particularly important to the structure with the 3-ML QW. There is a wide range of VBO values (from 0.12 to 0.9 eV) reported in the past [10]-[13]. Our study has narrowed significantly the VBO range. Previously, Ledentsov et. al. have compared the measured transition energies of thin GaSb layers with their theoretical calculations, and found a large discrepancy [3]. This is most likely due to a choice of a large VBO.

Antimony-mediated growth of high Indium composition InGaAs quantum well on InP substrate

在磷化銦基板上成長二維電子氣（2DEG）結構，要成長高品質 10 nm 平坦之砷化銦鎵通道層，受限於壓縮應力其銦含量很難超過 70%。欲超過 70%之銦含量，成長溫度必須低於 450℃以增加臨界厚度[14]，但單晶之品質卻被犧牲了，電子遷移率仍舊無法有效提高。對於壓縮應力下砷化銦鎵的單晶成長，銻原子可作為介面活性劑（surfactant）以增加其臨界厚度。以有機金屬化學汽相沈積為磊晶技術，銻原子的介面活性效應已經被利用來實現高銦含量（80%）砷化銦鎵長波長（室溫 2.1 μm）量子井雷射 [15]。

在本計畫中，我們使用分子束磊晶系統，將銻原子之介面活性效應用在 2DEG 結構中來成長高銦含量之電子通道層。我們檢視在高度壓縮應變之 InGaAs 磊晶層中不同 Sb 摻雜量對其表面形貌，光學特性以及電子遷移率的影響。樣品是用分子束磊晶技術，成長於 InP 基版上。首先成長 500nm 晶格匹配的 $In_{0.52}Al_{0.48}As$ 緩衝層，接著是 5nm 晶格匹配的 $In_{0.53}Gs_{0.47}As$ 能障層，再來就是 10nm 高壓縮應變的 $In_{0.83}Gs_{0.17}As$ 量子井通道層。其中 83%的銦含量是由 X-ray 繞射技術來鑑定。接著成長 25nm 晶格匹配的 Si delta-doped $In_{0.52}Al_{0.48}As$ 來給予通道載子，其中 delta-dope 的位置是在通道介面上方 5nm 處。為了檢視 Sb 介面活性效應對 $In_{0.83}Gs_{0.17}As$ 通道層電子遷移率的影響，我們成長了五片不同程度摻雜 Sb 的樣品。其 Sb 摻雜量由少到多依序為 0, 2×10^{-8} torr, 6×10^{-8} torr, 1×10^{-7} torr, 1.3×10^{-7} torr。針對無摻雜與摻雜 6×10^{-8} torr 的樣品，我們也另外成長了供原子力顯微鏡掃瞄用的樣品，其 1x 1 μm^2 尺寸的掃瞄影像如圖五所示。明顯地，摻雜 Sb 的樣品其表面比起無摻雜的要平坦許多。無摻雜的 $In_{0.83}Gs_{0.17}As$ 薄膜因為承受不了累積之壓縮應力，產生了落差約 30 nm 的表面粗糙結構。由於此粗糙結構伴隨著許多的

差排錯位於單晶中，造成大量的非輻射中心，樣品之光學特性將大幅下降，此結果可以由圖六觀察到。圖六為此五個樣品的 20K 光激發光圖，其發光強度隨著 Sb 的摻雜量先大幅度提升至飽和，而後緩慢下降。我們發現 Sb 的摻雜量不能太少也不能太多，6×10^{-8} torr 摻雜量是 $In_{0.83}Gs_{0.17}As$ 薄膜品質最好，其發光強度比起無摻雜的樣品高出約 180 倍。我們把此五樣品的光譜峰值位置與電子霍爾遷移率對摻雜量做圖，如圖三所示。我們發現，室溫下的電子遷移率也是隨著 Sb 之摻雜先大幅度上升，而後略微下降。究其原因，我們認為 Sb 在低於 6×10^{-8} torr 的摻雜量時主要是作為介面活性劑來幫助 $In_{0.83}Gs_{0.17}As$ 薄膜的成長，本身並無增加薄膜的應力。當 Sb 摻雜量大於 6×10^{-8} torr 時，Sb 本身也加入 $In_{0.83}Gs_{0.17}As$ 薄膜的成長，增加了薄膜應力使得單晶品質劣化，所以電子遷移率與發光強度均開始衰減。圖七顯示的頻譜峰值位置隨 Sb 摻雜量的趨勢圖也支持這個想法。在 Sb 摻雜量低於 6×10^{-8} torr 時峰值並無明顯紅移，表示 Sb 並未加入薄膜中。當摻雜量高於 6×10^{-8} torr 時，Sb 材料的加入使得薄膜發光頻譜開始紅移。我們發現最適當的 Sb 摻雜量為剛開始促使光譜紅移時的量，此時通道之室溫電子遷移率可達 12500 $cm^2/V*sec$。

Reference:

1. Yasuhiro Oda, Haruki Yokoyama, Kenji Kurishima, Takashi Kobayashi, Noriyuki Watanabe, and Masahiro Uchida, Appl. Phys. Lett. **87**, 023503 (2005)
2. Q. Yang, C. Manz, W. Bronner, Ch. Mann, L. Kirste, K. Kohler, J. Wanger, Appl. Phys. Lett. **86**, 131107 (2005)
3. N. N. Ledentsov, J. Bohrer, M. Beer, F. Heinrichsdorff, M. Grundmann, D. Bimberg, S. V. Ivanov, B. Ya. Meltser, S. V. Shaposhnikov, I. N. Yassievich, N. N. Faleev, P. S. Kop'ev, and Zh. I. Alferov, Phys. Rev. B **52**, 14058 (1995)
4. F. Hatami, N. N. Ledentsov, M. Grundmann, J. Bo¨hrer, F. Heinrichsdorff, M. Beer, D. Bimberg, S. S. Ruvimov, P. Werner, U. Go¨sele, J. Hexdenreich,U. Richter, S. V. Ivanov, B. Ya. Meltser, P. S. Kop'ev, and Zh. I.Alferov, Appl. Phys. Lett. **67**, 656 (1995)
5. C.-K Sun, G. Wang, J. E. Bowers, B. Brar, H,-R. Blank, H. Kroemer, and M. H. Pilkuhn, Appl. Phys. Lett. **68**, 1543 (1996)
6. M.Hayne, J. Maes, S. Bersier, M. Henini, L. Muller-Kirsch, Rober Heitz, D. Bimberg, V. V. Moshchalkov, Phisica B **346-347**, 421 (2004)
7. Makoto Kudo, Tomoyoshi Mishima, Satoshi Iwamoto, Toshihiro Nakaoka, Yasuhiko Arakawa, Physica E **21**, 275 (2004)
8. A. Zakharova, S. T. Yen, and K. A. Chao, Phys. Rev. B **66**, 085312 (2002)
9. I. Vurgaftman, J. R. Meyer, and L. R. Ram-Mohan, J. Appl. Phys. **89**, 5815 (2001)
10. A. D. Katnani, and G. Margaritondo, J. Appl. Phys. **54**, 2522 (1983)
11. J. Tersoff, Phys. Rev. B **30**, 4874 (1984)
12. Y. Tsou, A. Ichii, and Elsa M. Garmire, IEEE J. Quantum Electron. **28**, 1261(1992)
13. F. L. Schuermeyer, P. Cook, E. Martinez, and J. Tantillo, Appl. Phys. Lett. **55**, 1877 (1989)
14. X. Wallart, B. Pinsard, and F. Mollot. J. Appl. Phys. **97,** 053706 (2005)
15. Tomonari Sato, Manabu Mitsuhara, Takao Watanabe, and Yasuhiro Kondo. Appl. Phys. Lett. **87**, 211903 (2005)

Figure caption:

Figure 1: AFM surface images of (a) sample A (with 5um square image area), and (b) sample B (with 1um square image area).

Figure 2: Photoluminescence spectra of (a) sample A, and (b) sample B at 15K.

Figure 3: The measured transition energy vs. the cubic root of the excitation power. The interceptions of the extrapolated lines with the *y*-axis give the transition energies at thermal equilibrium. The carrier transition diagram for a GaSb/GaAs quantum well is shown in the inset.

Figure 4: The transition energies of quantum wells with 1ML, 2ML and 3ML of GaSb. The measured result is compared with the theoretical result.

Figure 5: AFM surface image of (a) 10nm $In_{0.83}GaAs$ without antimony doping. (B) 10nm $In_{0.83}GaAs$ with 6×10^{-8} torr antimony. (the image size is 1um square)

Figure 6: The low temperature PL signal of the samples.

Figure 7: The room temperature electron mobility and the antimony doping amount.

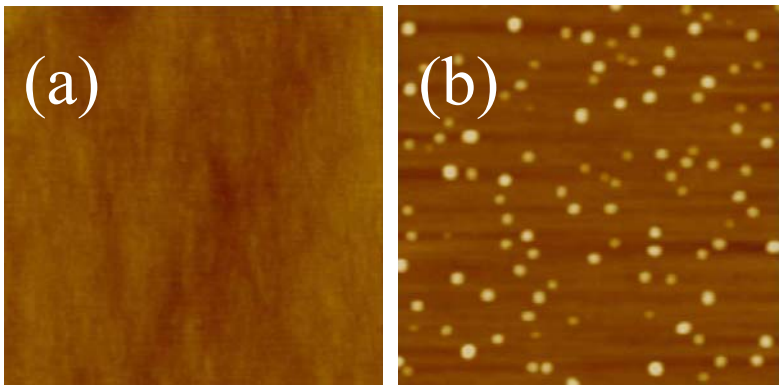

Figure 1

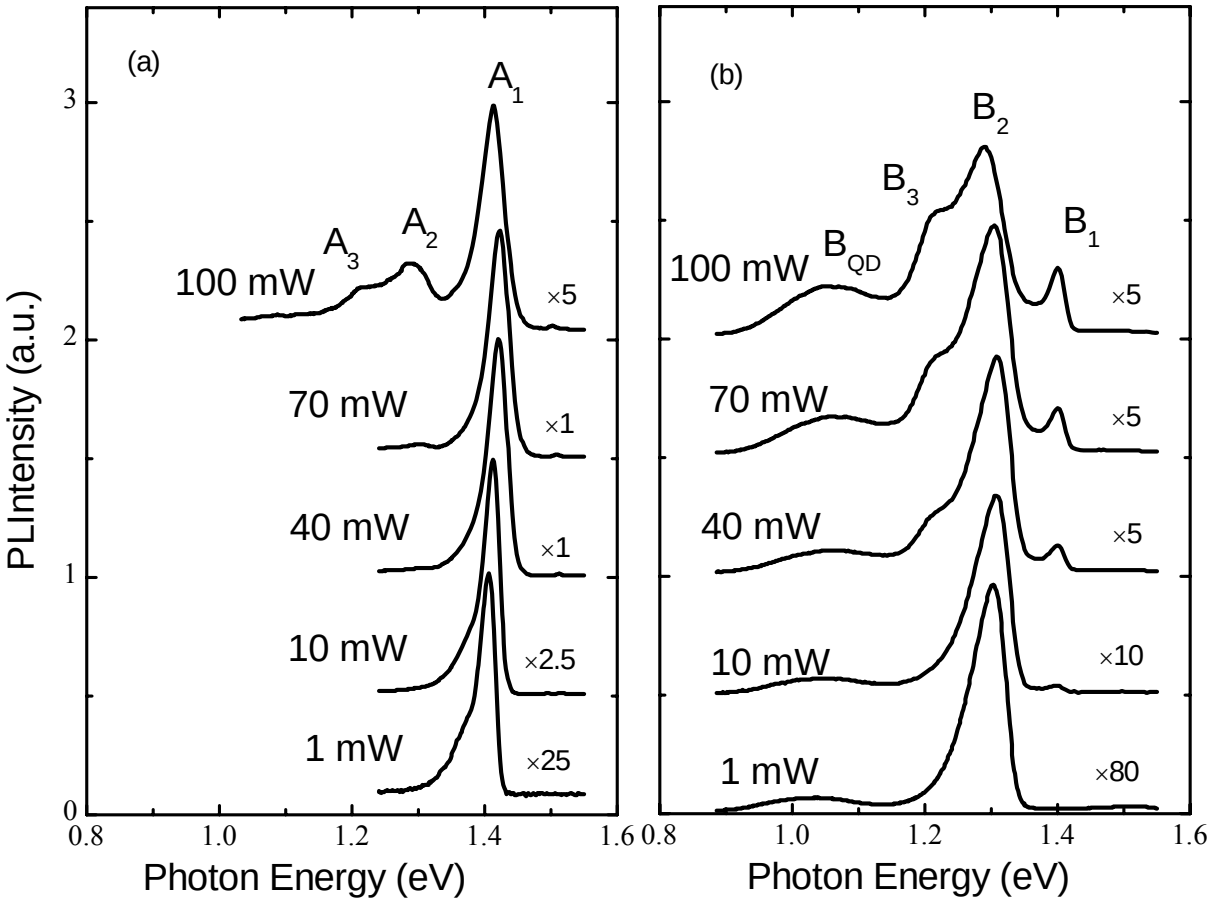
(a)
(b)
A1
A2
A3
B1
B2
B3
BQD
100 mW
70 mW
40 mW
10 mW
1 mW
×5
×1
×2.5
×25
×10
×80
PLIntensity (a.u.)
Photon Energy (eV)
0
1
2
3
0.8
1.0
1.2
1.4
1.6

Figure 2

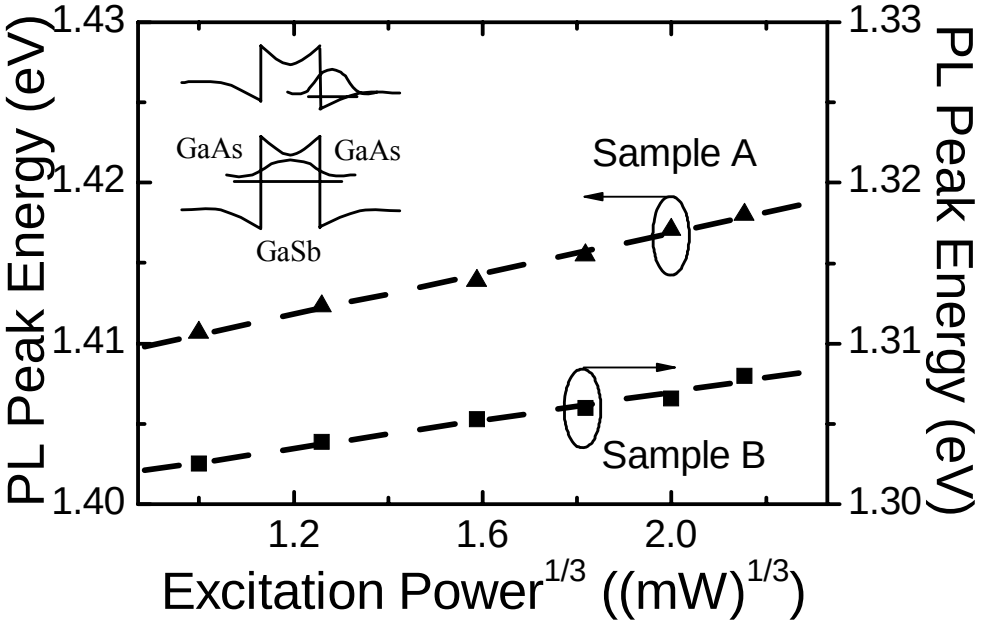
1.43
1.42
1.41
1.40
1.33
1.32
1.31
1.30
PL Peak Energy (eV)
PL Peak Energy (eV)
GaAs
GaAs
GaSb
Sample A
Sample B
1.2
1.6
2.0
Excitation Power^1/3 ((mW)^1/3)

Figure 3

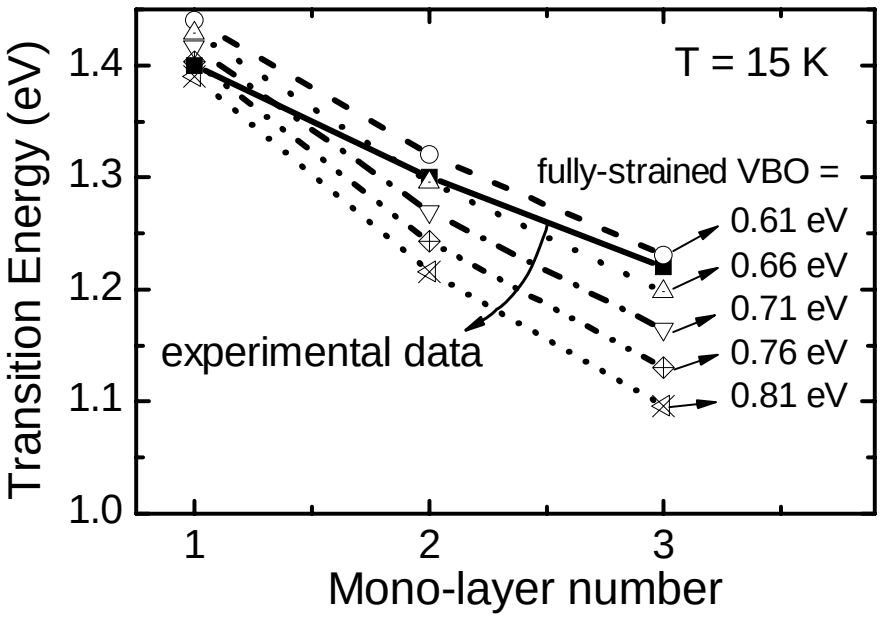
T = 15 K
fully-strained VBO =
0.61 eV
0.66 eV
0.71 eV
0.76 eV
0.81 eV
experimental data
Transition Energy (eV)
1.4
1.3
1.2
1.1
1.0
1
2
3
Mono-layer number

Figure 4

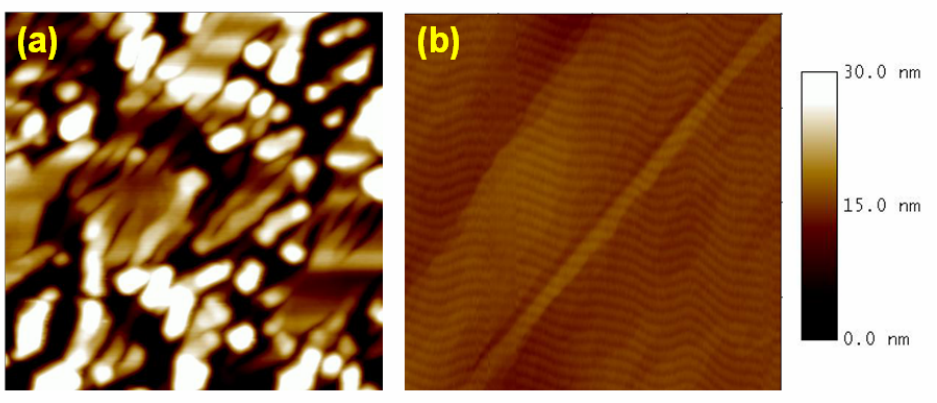

Figure 5

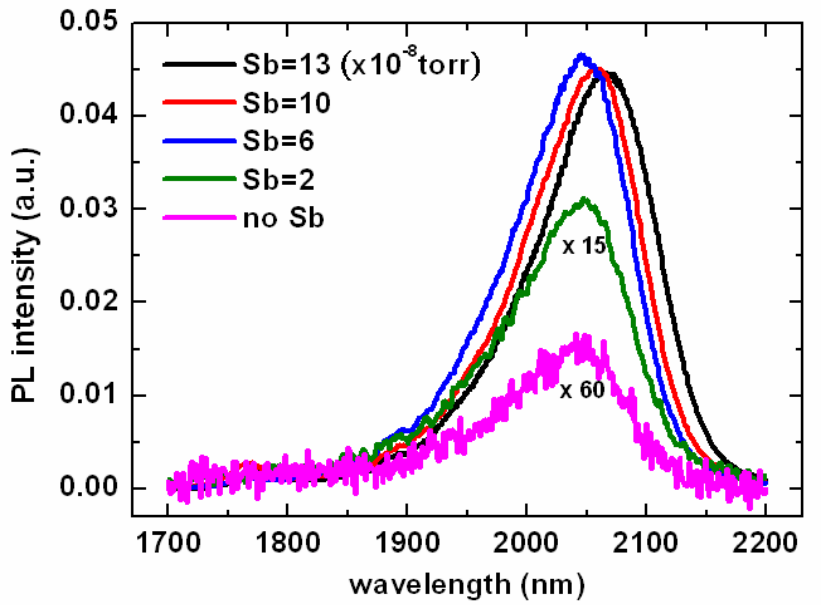
0.05
0.04
0.03
0.02
0.01
0.00
PL intensity (a.u.)
Sb=13 (x10^-8torr)
Sb=10
Sb=6
Sb=2
no Sb
x 15
x 60
1700
1800
1900
2000
2100
2200
wavelength (nm)

Figure 6

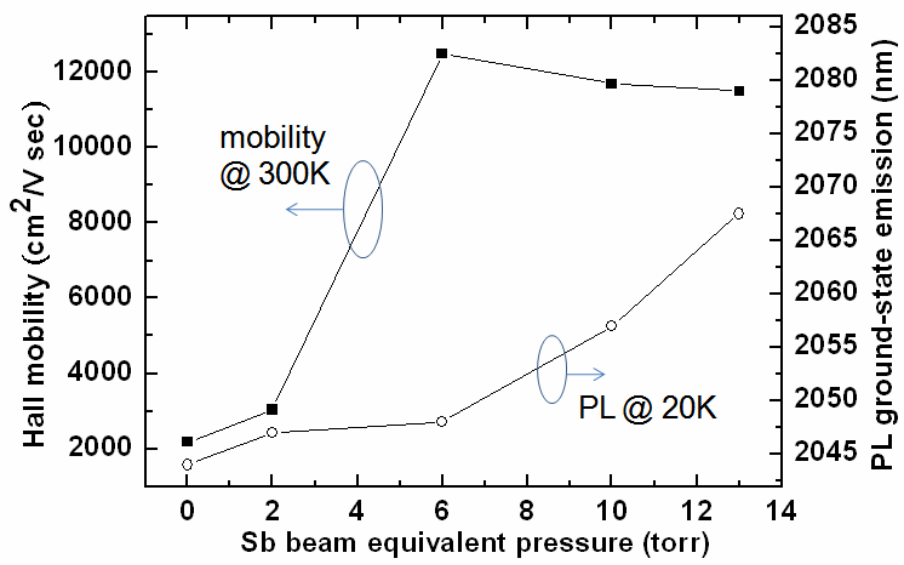
Hall mobility (cm^2/V sec)
PL ground-state emission (nm)
Sb beam equivalent pressure (torr)
mobility
@ 300K
PL @ 20K
2000
4000
6000
8000
10000
12000
2045
2050
2055
2060
2065
2070
2075
2080
2085
0
2
4
6
8
10
12
14

Figure 7